REPUBLIC OF AZERBAIJAN

On the rights of the manuscript

ABSTRACT

of the dissertation for the degree of Doctor of Philosophy

DESCRIPTION OF PROMPT PHOTON PRODUCTION IN THE NICA SPD EXPERIMENTAL SET-UP

Speciality:	2212.01 Theoretical physics
Field of science:	Physics
Applicant:	**Mohsun Rasim oglu Alizada**

Baku – 2025

The work was performed at the Department of Theoretical Physics, Baku State University, Ministry of Science and Education of Azerbaijan Republic and at the N.N.Bogolyubov Laboratory of Theoretical Physics, Joint Institute for Nuclear Research, Dubna, Russia.

Scientific supervisors: doctor of sciences, professor
Azar Inshalla oglu Ahmadov

doctor of physical and mathematical sciences, professor of Russian AS Sciences
Andrey Borisovich Arbuzov

Official opponents: doctor of science on physics
Mirteymur Mirkazim oglu Mirabutalibov

doctor of physical and mathematical sciences
Mais Kazim oglu Suleymanov

candidate of physical and mathematical sciences, associated professor
Bahram Isak oglu Mehdiyev

Dissertation council ED 2.19 of Supreme Attestation Commission under the President of the Republic of Azerbaijan operating at the Baku State University

Chairman of the Dissertation council:
____________ doctor of science on physics
Huseyn Mikayil oglu Mammadov

Scientific secretary of the dissertation council:
____________ doctor of philosophy in physics
Shahla Nabi gizi Hajiyeva

Chairman of the scientific seminar:
____________ doctor of physical and mathematical sciences, professor
Sarhaddin Gubaddin oglu Abdullayev

GENERAL CHARACTERISTICS

Relevance and degree of development of the topic. Prompt photons play a crucial role in studying high-energy hadronic and nuclear interactions. Being color-neutral, they have a large mean free path not only in dense hadronic matter but also in the quark-gluon plasma (QGP). This ensures that if they are produced at any stage, they exit the interaction region unchanged and can be detected. The study of prompt photon production is particularly important for determining the gluonic component of hadrons, as photons carry information about hard subprocesses.[1]

Previously, prompt photon production processes were studied in experiments at the Large Hadron Collider (LHC, CERN) and the American Tevatron during proton-proton, heavy-ion (p-Au, p-Pb, Au-Au, Pb-Pb) collisions. Numerous theoretical and experimental works focus on the dependence of the differential cross-section (DS) on kinematic parameters: the energy of colliding particles ($\sqrt{s}$), transverse momentum (p_T), cosine of the scattering angle ($Cos(\theta)$), rapidity (y), and the parameter x_T [2].

However, the high collision energies at the LHC and Tevatron lead to the production of many secondary particles, including thermal photons, complicating the precise determination of the prompt photon DS [3]. This limits the ability to study the dynamic structure of colliding nucleons and parton distributions. In this regard, experiments planned at the NICA collider offer significant advantages, as the col-

---

[1] Aad, G. on behalf of the ATLAS Collaboration Measurements of the inclusive and differential production cross sections of a top-quark-antiquark pair in association with a Z boson at $\sqrt{s}$=13 TeV with the ATLAS detector // Eur. J. Phys. C, – 2021. Aug; v. 81. – p. 1-43.

[2] Saimpert, M. on behalf of the ATLAS Collaboration Measurement of the inclusive photon and photon+jet production cross-sections at $\sqrt{s}$= 7 TeV with the ATLAS detector and constraints to PDFs // The XXIII International Workshop on Deep Inelastic Scattering and Related Subjects, – Dallas: Texas, USA, – 2015. – p. 1-8.

[3] Adare, A. on behalf of the PHENIX Collaboration Observation of direct-photon collective flow in $\sqrt{s_{NN}}$=200 GeV Au–Au Collisions // Phys. Rev. Lett., – 2012, v. 109, – p. 122302-1-7.

lision energy of heavy ions ($\sqrt{s}$=10 GeV) reduces the number of additionally produced particles. The energy of 10 GeV is also interesting because it bridges the gap between perturbative QCD (pQCD) and the physics of bound states and resonances, offering insights into the problem of quark confinement and phase transitions [4]. Thus, studying prompt photon production processes at NICA energies is highly relevant.

Object and subject of research. The object of research is prompt photons produced in proton-proton collisions at NICA energies. The subject of the dissertation is the dependence of the DS of prompt photon production on kinematic parameters: the energy of colliding protons ($\sqrt{s}$), transverse momentum (p_T), cosine of the scattering angle ($Cos(\theta)$), rapidity (y), and the parameter x_T.

Purpose and objectives of the study. The aim of this thesis is to investigate prompt photons production in subprocesses of Compton scattering of quark-gluon $qg \to q\gamma$, annihilation of the quark-antiquark pair $q\bar{q} \to g\gamma$ and bremsstrahlung $qq \to qq\gamma$ in proton-proton collisions at NICA energies and determination of the dominant process. Study of the influence of the longitudinal polarization of colliding protons on the DS of prompt photon production.

In order to achieve the objective, the following objectives were addressed:

1. Calculation of DS of the subprocesses of Compton scattering of quark-gluon and annihilation of quark-antiquark pair in the leading order of perturbation without polarization and taking into account the longitudinal polarization of colliding particles;

2. Calculation of DS of the subprocesses of Compton scattering of quark-gluon and annihilation of quark-antiquark pair in the next-to-leading order of perturbation without polarization and taking into account the longitudinal polarization of colliding particles;

3. Calculation of contributions of radiative corrections to the subprocesses of Compton scattering of quark-gluon and annihilation of quark-antiquark pair production of prompt photons in proton-proton collision,

---

[4] NICA physics: [Electronic resource] / URL: https://nica.jinr.ru/physics.php.

4. Calculation of DS of prompt photon production in proton-antiproton collisions without polarization and taking into account the longitudinal polarization of colliding particles.

Research methods. The Feynman diagram technique and quantum field theory methods were used in the course of the work. Feynman diagrams were constructed with the program FeynArt, matrix elements and square of module of the matrix element were calculated in FeynCalc, the DS was calculated in Mathmetica-10 environment, graphs were constructed in Origin 8.5 and edited in Adobe Photoshop 8.

The main provisions for defense:

1. The contribution of Compton scattering of quark-gluon subprocess to the total DS of the prompt photon production process in proton-proton collisions decreases with increasing energy of colliding protons $\sqrt{s}$. However, this subprocess remains dominant also at NICA energies;

2. The longitudinal polarization of colliding protons does not change the character of the dependences of the DS on the kinematic parameters of the processes. It affects differently the DS of the subprocesses of Compton scattering of quark-gluon, annihilation of quark-antiquark pair, and bremsstrahlung;

3. The contributions of calculations next-to-leading order perturbation are significant at high energies of colliding protons. The longitudinal polarization of colliding protons significantly affects the DS of prompt photons production calculated next-to-leading order perturbation;

4. The contributions of radiative corrections to Compton scattering of quark-gluon subprocess are larger than the contributions of radiative corrections to the annihilation of quark-antiquark pair subprocess;

5. The DS of prompt photons production in the proton-antiproton collision is larger than in the proton-proton collision. At energies $\sqrt{s}$=10 GeV the proton-antiproton and proton-proton collisions can be considered identical.

Scientific novelty of the research:

1. The DS of the subprocesses of Compton scattering of quark-gluon $qg \to q\gamma$, annihilation of quark-antiquark pair $q\bar{q} \to g\gamma$ and bremsstrahlung of quarks $qq \to qq\gamma$ of the prompt photons production in proton-proton collisions at NICA energies were determined in the leading and next-to-leading order of perturbation without polarization and taking into account the longitudinal polarization of colliding protons;

2. The contributions of radiative corrections to the subprocesses of Compton scattering of quark-gluon and annihilation of quark-antiquark pair of the prompt photons production have been calculated;

3. The DS of prompt photons production in proton-antiproton collisions without polarization and taking into account the longitudinal polarization of colliding particles and the effect of sea and valence quarks on the DS are determined.

Theoretical and practical significance of the research. At NICA energies, parton distribution functions (PDF) from the LHC and Tevatron can be used. Accounting for longitudinal proton polarization does not alter the dependence of DS on kinematic parameters.

The results are applicable for describing promptt photon production in low-energy proton-proton collisions, particularly for experiments at NICA. They are also useful for studying proton structure, constraining PDF in a new kinematic region (x, Q^2), and reducing systematic uncertainties in Monte Carlo modeling.

Approbation and application. Materials of the dissertation work were reported and discussed at:

– seminars of the department of Theoretical Physics of Baku State University;

republican conferences:

– Azerbaycan Respublikasi Tehsil Nazirliyi, Baki Dovlet Universiteti, Magistrantlarin ve genc tedqiqatchilarin "SHUSHA ILI"-ne hesr olunmus "Fizika ve Astronomiya Problemleri" adli XXII Umumrespublika elmi konfransi, – Baki: – May 20, – 2022 (in Azerbaijan);

– Umummilli Lider Heydar Aliyevin anadan olmasinin 99-cu ildonumune hesr olunmus Genc Tedqiqatchilarin VI Beynelxalq Elmi Konfransi, – Baki: – Aprel 29-30, – 2022 (in Azerbaijan);

– Doktorantlarin ve genc tedqiqatchilarin XXV Respublika elmi konfransi, Baki Muhendislik Universiteti, Baki, – Noyabr 23-24, – 2022 (in Azerbaijan);

– Umummilli Lider Heydar Aliyevin anadan olmasinin 100 illik yubileyine hesr olunmus "Fizika ve Astronomiyanin Problemleri" movzusunda Magistrantlarin ve Genc Tedqiqatchilarin XXIII Respublika elmi konfransi, Baki, – May 25, – 2023 (in Azerbaijan);

international conferences:

– The 7th International conference MTP-2021, Modern Trends in Physics, Baku State University, – Azerbaijan: Baku: – December 15-17, – 2021;

– The 2nd International Science and Technology Conference, Baku Engineering University, – Azerbaijan: Baku: – November 26-27, – 2021;

– LXXII International Conference "Nucleus-2022: Fundamental problems and applications", – Moscow: – July 11-16, – 2022;

– The XXVI International Scientific Conference of Young Scientists and Specialists, AYSS-2022, – Moscow: Dubna: – October 24-28, – 2022;

– The 21st Lomonosov Conference on Elementary Particle Physics, Moscow State University, – Moscow: – August 24-30, 2023;

– The 8th International conference MTP-2023, Modern Trends in Physics, Baku State University, – Baku: – December 15-17, – 2023;

– V International Applied Statistics Congress, UYIK-2024, – Istanbul: – May 21-23, – 2024;

– International conference on Computer science and gravitation, – Baku: – August 19-23, – 2024.

Publications. On materials of dissertation 21 works are published, including 6 in the form of articles in periodicals domestic recommended by the Higher Attestation Commission of the Republic of Azerbaijan, and 2 foreign journals, indexed in bases SCOPUS, Web of Science, 4 articles in materials of republican and 2 articles in materials of international conferences, indexed in bases SCOPUS, Web of Science and 7 theses in collections of republican and international conferences.

Name of the organization in which the dissertation work was carried out. The dissertation work was carried out at the Department of Theoretical Physics, Baku State University, Ministry of Science and Education of Azerbaijan Republic and the N.N.Bogolyubov Theoretical Laboratory, Joint Institute for Nuclear Research, Dubna, Russia.

The total volume of the dissertation in characters with indication of the volume of its structural sections separately. The dissertation work consists of an “Introduction", 5 chapters, a “Conclusions", a “List of references“ and a "List of abbreviations and symbols”. The total volume of work, together with 2 tables, 283 figures and a list of references, including 172 titles, is 241 pages. The total volume of the thesis, taken with a sign (excluding spaces, tables, graphs and a list of references), is 210552 characters (including Introduction – 14651, Chapter I – 59836, Chapter II – 51991, Chapter III – 35447, Chapter IV – 45031, Chapter V – 22870, the results are 3596 characters).

Author’s personal contribution. The author calculated DS for direct photon production subprocesses (quark-gluon Compton scattering and quark-antiquark annihilation) at leading and next-to-leading orders. Dependencies on $\sqrt{s}$, p_T, $Cos(\theta)$, y, x_T were determined and compared. Radiative corrections and DS for proton-proton and proton-antiproton collisions were computed. The author participated in task formulation, calculations, result discussions, and preparation of publications.

CONTENT OF THE WORK

The introduction substantiates the relevance of the work, provides information about its goals and objectives, scientific novelty, the main provisions submitted for defense, approbation of the results and publications.

The first chapter reviews theoretical and experimental studies of prompt photon production subprocesses ($qg \to q\gamma$, $q\bar{q} \to g\gamma$, $qq \to qq\gamma$) at the LHC and Tevatron. The advantages of experiments at NICA, particularly with polarized protons, are highlighted for studying the phase transition of QGP to hadronization. The possibility of determining the type and temperature of the phase transition in NICA experiments is noted. The chapter also describes the methods used: Feynman diagrams, quantum field theory, and software tools such as Mathematica, FeynArts, and FeynCalc.

The second chapter is devoted to calculations of the DS at leading order (LO) of the subprocesses of Compton scattering of quark-gluon $qg \to q\gamma$, annihilation of quark-antiquark pair $q\bar{q} \to g\gamma$ and bremsstrahlung $qq \to qq\gamma$ production of prompt photons in proton-proton collisions at NICA energies with unpolarized and longitudinally polarized of colliding protons.

1. DS of subprocess of Compton scattering of quark-gluon $qg \to q\gamma$ with unpolarized colliding protons.

Figure 1(a,b) shows Feynman diagrams of the subprocess of Compton scattering of quark-gluon $qg \to q\gamma$ production of prompt photons in the proton-proton collision.

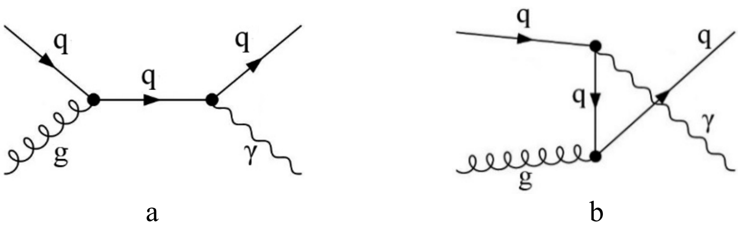

Figure 1 (a, b).

Mandelshtam invariants for Compton scattering $q(p_1) + g(k_1) \to q(p_2) + \gamma(k_2)$ subprocess have the following form:

$$\hat{s} = (k_1 + p_1)^2,\ \hat{t} = (k_1 - k_2)^2 \text{ and } \hat{u} = (p_1 - k_2)^2.$$

The square of the matrix element is equal to:

$$|\bar{M}|^2 = -\frac{16\pi^2\alpha\alpha_s}{3} \cdot \frac{\hat{u}^2 + \hat{s}^2}{\hat{u}\hat{s}}.$$

The DS of the subprocess is calculated by the formula[5,6]:

$$\frac{d\hat{\sigma}(qg \to q\gamma)}{d\hat{t}} = \frac{1}{16\pi\hat{s}^2}|\bar{M}|^2.$$

To transition the calculations from parton level to hadronic level, we used the parton distributions function CT14QED – $G_{q_1/h_1}(x_1)$[7]. At the hadron level, for the DS we obtain the following formulas:

$$d\sigma = \int (-t) G_{q_1/h_1}(x_1) G_{q_2/h_2}(x_2) dx_1 dx_2 \frac{d\hat{\sigma}}{d\hat{t}} dy$$

$$\frac{d\sigma}{dy} = \int (-t) G_{q_1/h_1}(x_1) G_{q_2/h_2}(x_2) dx_1 dx_2 \frac{d\hat{\sigma}}{d\hat{t}}. \quad (1)$$

$$\frac{d\sigma}{dp_T^2} = \int \left(\frac{-t}{2p_T^2}\right) G_{q_1/h_1}(x_1) G_{q_2/h_2}(x_2) dx_1 dx_2 \frac{d\hat{\sigma}}{d\hat{t}}$$

Figure 2(a,b,c,d,e) shows the dependence of total cross-section of Compton scattering of quark-gluon subprocess on the sum of energy of the colliding protons $\sqrt{s}$ and dependences of DS on transverse momentum p_T, the cosine of the scattering angle of the photon Cos(θ), the photon rapidity y and x_T[5].

As seen in Figure 2(a), the total cross-section increases with $\sqrt{s}$, reaching a maximum at $\sqrt{s} = 4.6$ GeV, after which it decreases. This is explained by the reduction in interaction time as particle velocity (energy) increases, consistent with pQCD predictions.

Figure 2(b) shows that the DS rapidly decreases with increasing p_T. This is due to photons being more likely emitted at small angles

---

5 Alizade M.R., Akhmedov A.I., Arbuzov A.B. Issledovaniye pod prochessov $qg \to q\gamma$ i $q\bar{q} \to g\gamma$ rojdeniya pryamikh fotonov pri proton-protonnom stolknovenii // Transactions of Azerbaijan National Academy of Sciences, Physics and astronomy, – Baku: – 2021. N 5, – p.11-19, (in Russian).

6 Alizada M.R., Ahmadov A.I., Arbuzov A.B. Prompt photons production in proton-proton collision at high energies // Proceedings of the 7th International conference MTP-2021, Modern Trends in Physics, Baku State University, – Baku: Azerbaijan: – 2021, v. 1, December 15-17, – p.142-145.

7 Sampaio dos Santos, G. The color dipole picture for prompt photon production in pp and pPb collisions at the CERN-LHC / G. Sampaio dos Santos, G. Gil da Silveira, M.V.T. Machado // Eur. Phys. J. C, – 2020. v. 80, n. 9, – p. 812-1-13.

relative to the colliding quark, corresponding to smaller p_T values. At high p_T, photon production is suppressed by the strong coupling constant (α_s) and PDF. In pQCD, the probability of hard scattering decreases with increasing transferred momentum (in this case, p_T), explaining the rapid decline.

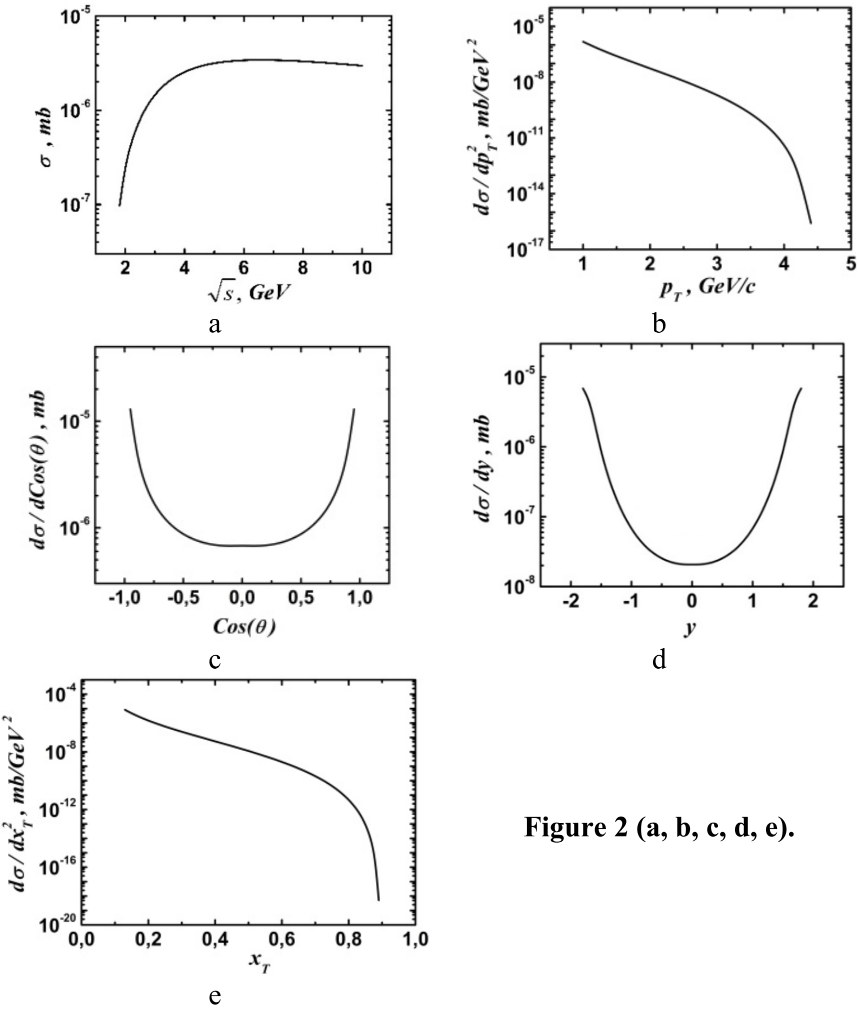

Figure 2 (a, b, c, d, e).

The dependence of the DS on Cos(θ) (Figure 2(c)) is symmetric around zero, with maxima near Cos(θ) ≈ ±0.95 and a minimum at

Cos(θ) = 0.

The dependence on photon rapidity (y) (Figure 2(d)) is also symmetric: maxima occur at extreme positive and negative y, with a minimum at $y = 0$. This indicates that the process is less probable when the quark and gluon have equal longitudinal momenta, leading to equal and opposite rapidities for the quark and photon.

The dependence on x_T (Figure 2(e)) shows a sharp decrease with increasing x_T, indicating a higher probability of the subprocess at low x_T. At low x_T, the photon has a small transverse momentum, meaning most of the subprocess energy is carried by the final quark. At high x_T, the photon carries most of the energy, making the subprocess less probable. This aligns with pQCD predictions that quarks and gluons interact more strongly at smaller relative momenta.

2. DS of subprocess of annihilation of a quark-antiquark pair $q\bar{q} \to g\gamma$ with unpolarized colliding protons.

Figure 3(a,b) shows Feynman diagrams of the subprocess of annihilation of quark-antiquark pair $q\bar{q} \to g\gamma$ production of prompt photons in the proton-proton collision.

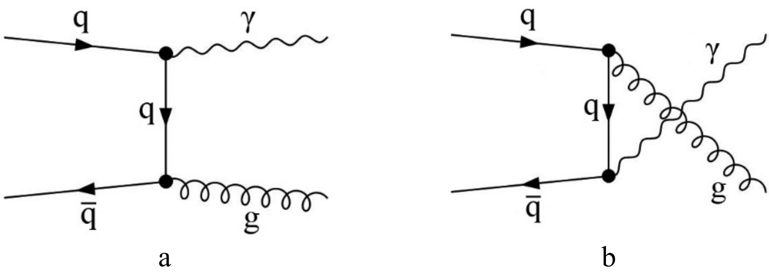

Figure 3 (a, b).

Mandelstam invariants for the subprocess $q(p_1) + \bar{q}(p_2) \to g(k_1) + \gamma(k_2)$ are as follows: $\hat{s} = (p_1 + p_2)^2$, $\hat{t} = (p_1 - k_1)^2$ и $\hat{u} = (p_2 - k_1)^2$. The square of the matrix element is equal to:

$$|\bar{M}|^2 = \frac{128\pi^2\alpha\alpha_s}{9} \cdot \frac{\hat{u}^2 + \hat{t}^2}{\hat{u}\hat{t}}.$$

DS of the annihilation of quark-antiquark pair $q\bar{q} \to g\gamma$ is equal to[5]:

$$\frac{d\sigma_{LO}}{dt} = \frac{1}{16\pi\sqrt{s[s-(m_1+m_2)^2]\cdot[s-(m_1-m_2)^2]}}|\bar{M}|^2.$$

Figure 4(a,b,c,d,e) shows the dependence of the total cross-section of annihilation of quark-gluon pair subprocess on the sum of energy of colliding protons $\sqrt{s}$ and dependences of DS on transverse

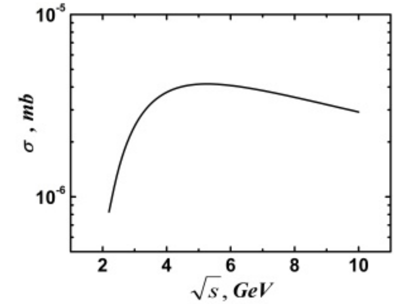

a

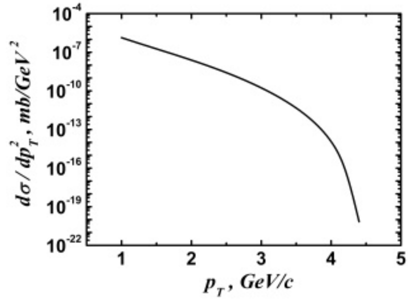

b

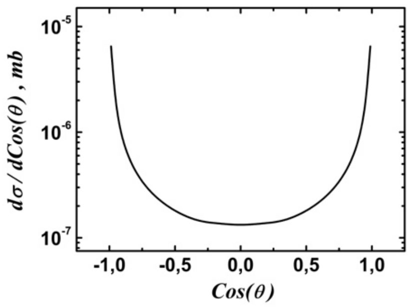

c

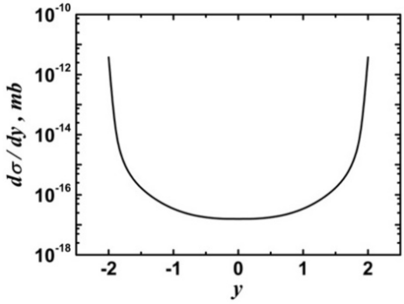

d

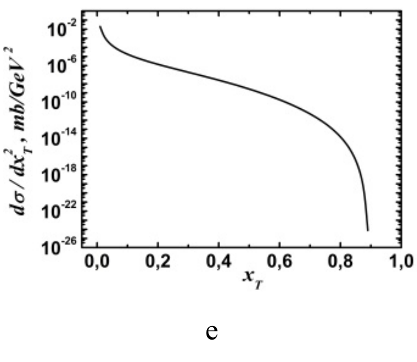

e

Figure 4 (a, b, c, d,e).

momentum p_T, the cosine of the scattering angle Cos(θ), the photon rapidity y, and the x_T.

From Figure 4(a), it is evident that at low energies, the total cross-section rapidly increases with $\sqrt{s}$, reaching a maximum at $\sqrt{s} = 5.2$ GeV, after which it slowly decreases. This is explained by the small relative velocity of the quark and antiquark at low energies, increasing the probability of gluon and photon production. At high energies, the cross-section is suppressed by the α_s of QCD.

The dependence on p_T (Figure 4(b)) shows exponential decay with increasing p_T. This is due to the suppression of PDFs of the quark and antiquark, which decrease with increasing parton momentum fraction. Additionally, the fragmentation function (FF) of the quark into a photon also influences this behavior.

The dependence on Cos(θ) (Figure 4(c)) is symmetric around zero, with maxima at $|\text{Cos}(\theta)| \approx 1$. This indicates that photon production is more probable in the forward or backward direction compared to perpendicular directions.

The dependence on rapidity (y) (Figure 4(d)) is symmetric, with maxima near $y = \pm 2$, corresponding to the gluon and photon being produced with equal and opposite rapidities.

The dependence on x_T (Figure 4(e)) shows a sharp decrease with increasing x_T, indicating that the process is more likely to occur when the produced gluon and photon have small transverse momenta.

3. DS of subprocess of bremsstrahlung $qq \to qq\gamma$ with unpolarized colliding protons.

Figure 5(a, b, c, d, e, f, g, h, i, j, k, l, m) shows the Feynman diagrams of subprocess of bremsstrahlung $qq \to qq\gamma$ production of prompt photons in the proton-proton collision.

Mandelstam invariants for the subprocess $q(p_1) + q(p_2) \to q(p_3) + q(p_4) + \gamma(k_1)$ are as follows[8,9]:

---

[8] Alizada M.R., Ahmadov A.I., Arbuzov A.B. Prompt photon production in the bremsstrahlung at NICA energies // Journal of Physics & Space Sciences, – Baku: Baku State University: – 2024, v 1 (2), – p. 43-49.

[9] Alizada M.R. Prompt photon production in bremsstrahlung from quark gluon plasma at $\sqrt{s}$=10 GeV energies // – Moscow: Bulletin of Moscow State University, Moscow: – 2024, v. 79, Suppl.1, S39-S41.

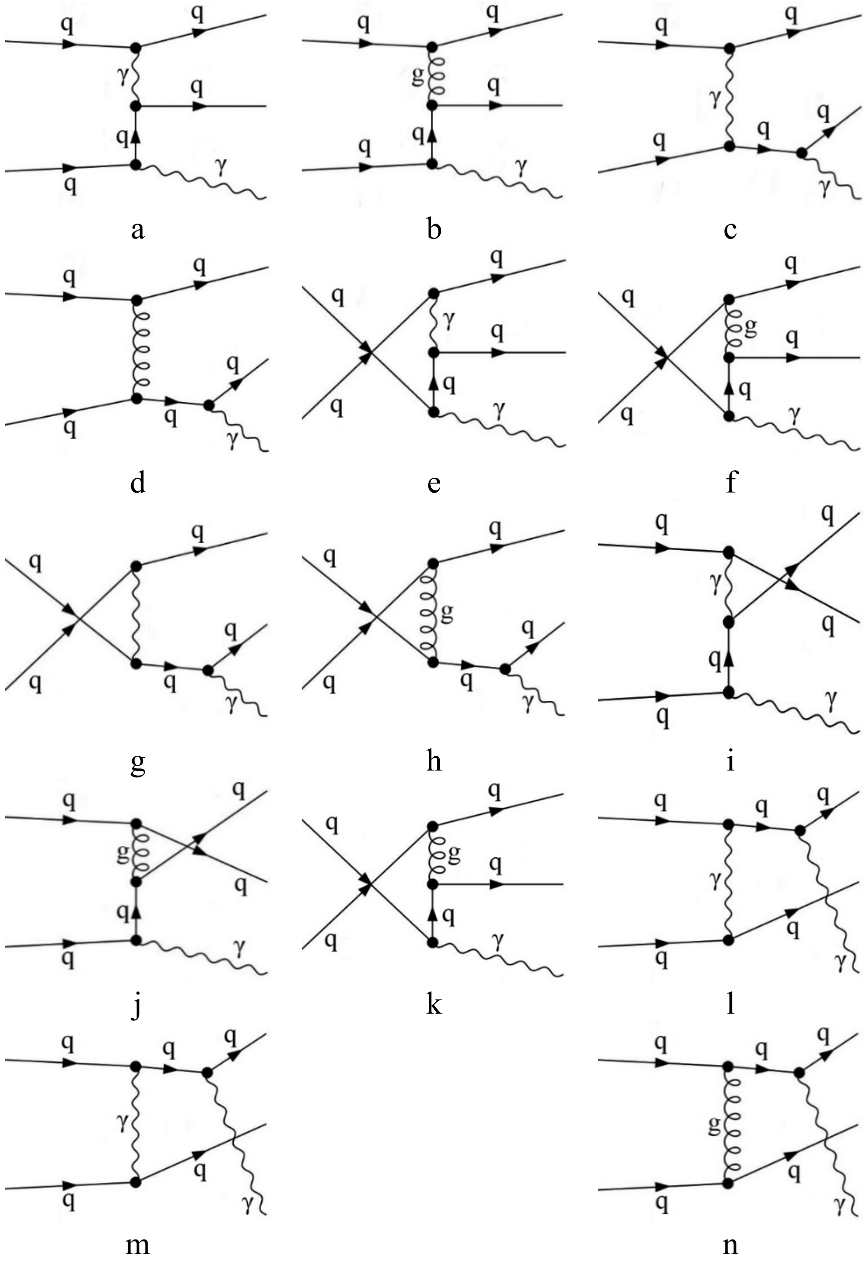

Figure 5 (a, b, c, d, e, f, g, h, i, j, k, l, m, n).

$$\hat{s} = (p_1 + p_2)^2 = (k_1 + p_3 + p_4)^2,$$
$$\hat{t} = (p_1 - k_1)^2 = (p_4 + p_3 - p_2)^2,$$
$$\hat{u} = (p_2 - k_1)^2 = (p_4 + p_3 - p_1)^2,$$
$$\hat{q}_1 = (p_1 - p_3)^2 = (k_1 + p_4 - p_2)^2,$$
$$\hat{q}_2 = (p_2 - p_4)^2 = (k_1 + p_3 - p_1)^2,$$
$$\hat{s}_1 = (p_4 + p_3)^2 = (p_1 + p_2 - k_1)^2,$$
$$\hat{t}_1 = (p_1 - p_4)^2 = (k_1 + p_1 - p_2)^2,$$
$$\hat{u}_1 = (p_2 - p_3)^2 = (k_1 + p_4 - p_1)^2,$$
$$\hat{q}_3 = (p_3 + k_1)^2 = (p_1 + p_2 - p_1)^2,$$
$$\hat{q}_4 = (p_4 + k_1)^2 = (p_1 + p_2 - p_3)^2.$$

A square matrix element was obtained, averaged over the spins of the inital particles and was used to compute the DS at the parton level:

$$\frac{d\hat{\sigma}(qq \to qq\gamma)}{d\hat{t}} = \frac{\hat{s}_1}{16\pi\hat{s}^4}|\bar{M}|^2.$$

Figure 6(a,b,c,d,e) shows the dependences of the total cross-section of the bremsstrahlung subprocess on the sum of energy of colliding protons $\sqrt{s}$ and the dependence DS on transverse momentum p_T, cosine of the scattering angle Cos(θ), photon rapidity, and x_T[10].

From Figure 6(a), it is evident that the DS of the bremsstrahlung process increases with the sum of energy of colliding protons. At high energies, partons inside the proton have high velocities, and their abrupt deceleration results in significant photon production. In the low-energy region ($\sqrt{s} < 3$ GeV), soft bremsstrahlung dominates, where the photon carries a small fraction of the quark's energy. In the intermediate region ($3<\sqrt{s} < 7$ GeV), radiation is enhanced due to collinear bremsstrahlung. In the high-energy region ($\sqrt{s} > 7$ GeV), the DS rapidly decreases due to the "dead cone" effect, which suppresses photon production in the direction of the quark.

Figure 6(b) presents the dependence of the DS on the transverse momentum of photons (p_T). The DS decreases rapidly with increasing p_T, as the probability of production of high-energy photon is low. As p_T approaches the kinematic limit $p_T = \sqrt{s}/2$, the DS tends to zero because photon production becomes kinematically forbidden when the final-state quarks have zero energy and momentum.

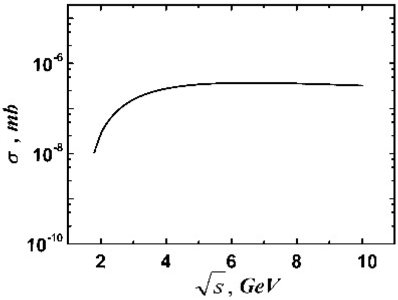

a

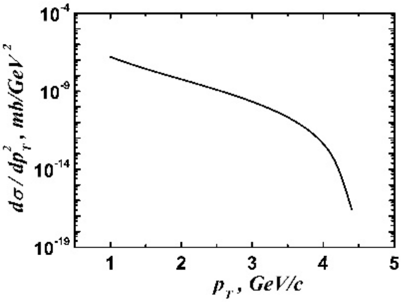

b

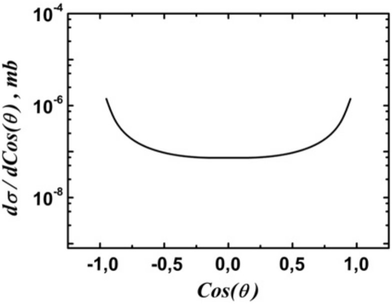

c

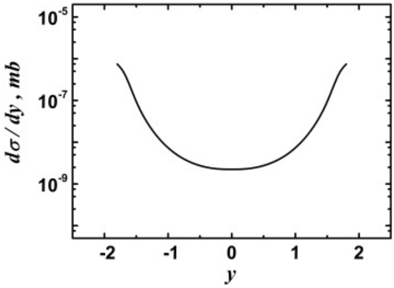

d

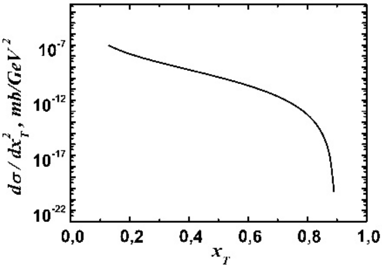

e

Figure 6 (a, b, c, d, e).

The dependence on the cosine of the scattering angle (Figure 6(c)) shows a symmetric bell-shaped curve. This indicates that the probability of photon production is minimal when the quarks scatter at a right angle ($Cos(\theta) = 0$) and maximal when they move in the same or opposite directions ($Cos(\theta) = \pm 1$). A similar pattern is observed for the dependence on rapidity (Figure 6(d)).

The dependence of the DS on x_T (Figure 6(e)) shows its rapid decrease with increasing x_T. This means that the probability of production of photon with high transverse momentum is much lower compared to a photon with low transverse momentum. This is consistent with the dependence of the DS on the transverse momentum of the produced prompt photons (p_T).

4. DS of subprocess of Compton scattering of quark-gluon $qg \to q\gamma$ with longitudinally polarized colliding protons.

Taking into account the polarization of the initial quark and gluon (photon), consequently, the product of four-dimensional spinors and four-dimensional polarization vectors were taken as[10]:

$$U(p_1)\bar{U}(p_1) = \frac{1}{2}(1 - \lambda_1\gamma_5)(\hat{p}_1 + m_1), \tag{2}$$

where λ_1 and λ_2 are the helicity of the colliding protons, m_1, m_2 are the masses of the quark and antiquark, $\hat{p}_1$, $\hat{p}_2$ are the momenta of the quark and antiquark, correspondingly.

To take into account the polarization of the initial gluon (photon), the four-dimensional vectors of the initial particles are written as

$$\hat{e}^{\lambda_2}(k_1) = \frac{(1 + \lambda_2\gamma^5)\hat{k}_2\hat{q}\hat{k}_1 + (1 - \lambda_2\gamma^5)\hat{k}_1\hat{q}\hat{k}_2}{4\sqrt{(k_1k_2)(k_1q)(k_2q)}}, \tag{3}$$

where λ_2 is the helicity of the initial gluon (photon).

The squared modules of matrix element, averaged over the spins of final particles and the DS of the process is given by:

$$|\bar{M}|^2 = -\frac{8\alpha_E\alpha_s e_q^2}{9}\left(\frac{\hat{s}}{\hat{u}}(1 - 2\lambda_1\lambda_2 + \lambda_2^2) + \frac{\hat{u}}{\hat{s}}(1 + 2\lambda_1\lambda_2 + \lambda_2^2)\right),$$

and

$$\frac{d\hat{\sigma}_{POL}(qg \to q\gamma)}{d\hat{t}} =$$

[10] Ji, Z. Measurement of direct photon cross section and double helicity asymmetry at $\sqrt{s}$= 510 GeV in $\vec{p} + \vec{p}$ collisions at PHENIX // JPS Conf. Proc., – 2022. v. 37, – p. 251901-1-8.

$$= -\frac{\alpha_s \alpha_e e_q^2}{18\pi \hat{s}^2}\left(\frac{\hat{s}}{\hat{u}}(1 - 2\lambda_1\lambda_2 + \lambda_2^2) + \frac{\hat{u}}{\hat{s}}(1 + 2\lambda_1\lambda_2 + \lambda_2^2)\right).$$

The double spin asymmetry at longitudinal polarization at the hadronic level is determined by the formula[11]:

$$A_{LL} = \frac{\sigma^{\uparrow\uparrow} - \sigma^{\uparrow\downarrow}}{\sigma^{\uparrow\uparrow} + \sigma^{\uparrow\downarrow}}, \tag{4}$$

where $\sigma^{\uparrow\uparrow}$ and $\sigma^{\uparrow\downarrow}$ are the cross-sections of the processes with parallel and antiparallel polarizations of the colliding protons, respectively.

At the parton level, the expression for the double spin asymmetry of the subprocess of Compton scattering of quark-gluon subprocess $qg \to q\gamma$ has the following expression:

$$\hat{A}_{LL} = \frac{2\lambda_1\lambda_2(\hat{u}^2 - \hat{s}^2)}{(\lambda_2^2 + 1)(\hat{u}^2 + \hat{s}^2)}. \tag{5}$$

As can be seen, the double spin asymmetry depends on both the helicities and the kinematic variables of the partons.

Figure 7(a,b,c,d,e) shows the dependences of the double spin asymmetries of the subprocess $qg \to q\gamma$, calculated at polarization order P_1, P_2=0.9, -0.9 (curve 1) and P_1, P_2=±0.9 (curve 2) from the sum of colliding particle energy $\sqrt{s}$ (a), transverse momentum of prompt photons p_T (b), rapidity y (c), x_T (d) and a three-dimensional plot of the dependence on the of polarization order P_1 and P_2 (e) at $\sqrt{s}$=10 GeV[12].

As seen in Figure 7(a), both curves asymptotically approach zero at high energies, indicating a small effect of longitudinal polarization on the DS at high energies.

---

[11] Kanazawa, Y. A_{LT} in the polarized Drell-Yan process at RHIC and HERA energies / Y. Kanazawa, Y. Koike, N. Nishiyama // Phys. Lett. B, – 1998. v. 430, – p. 195–202.

[12] Alizada M.R. Ahmadov A.I., Arbuzov A.B. Contribution of the QED compton scattering subprocess to prompt photon production in collisions of longitudinally polarized protons at NICA energies // Dubna: Physics of Particles and Nuclei Letters, 2025, Vol. 22, No. 2, pp. 6–17.

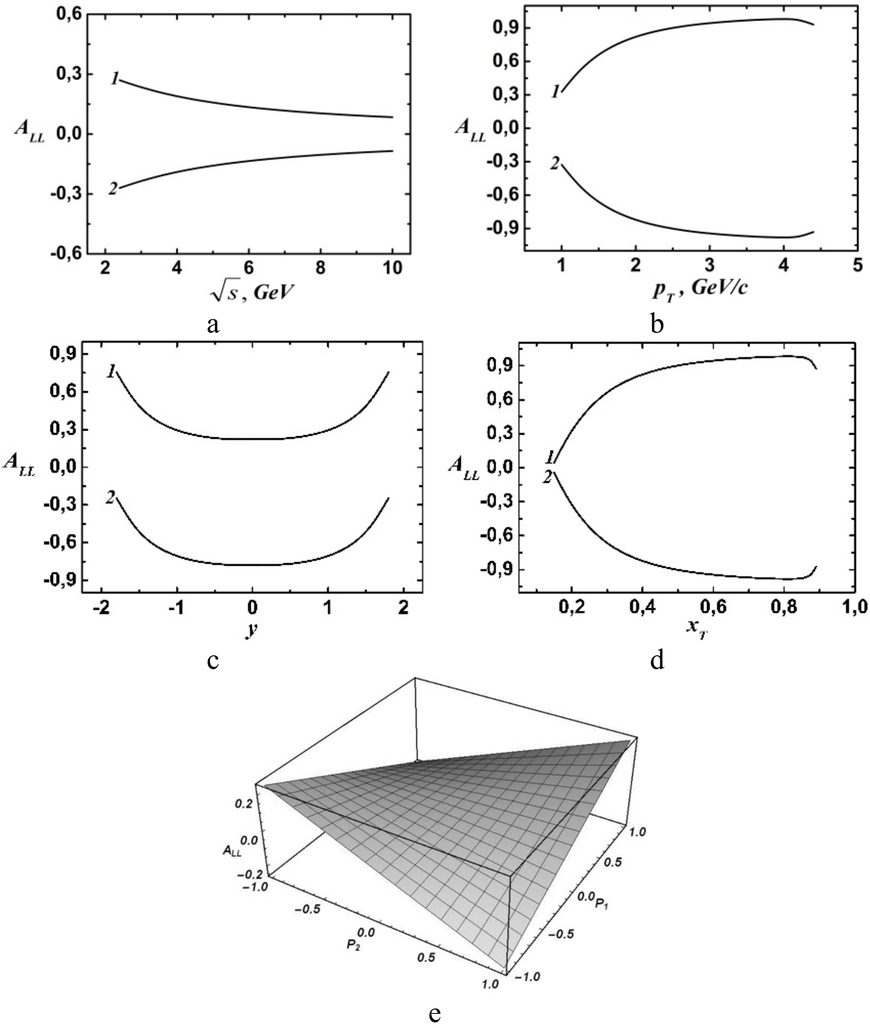

Figure 7 (a, b, c, d, e).

The dependence of A_{LL} on p_T and x_T (Figures 7(b) and 7(d)) shows that for $P_1, P_2 = 0.9, -0.9$, the asymmetry increases to saturation, while for $P_1 = P_2 = \pm 0.9$, it decreases.

The 3D plot (Figure 7(e)) shows that maximum asymmetry is achieved for opposite values of P_1 and P_2. This confirms the thesis that opposite polarization directions enhance spin effects.

5. DS of subprocess of annihilation of quark-antiquark pair $q\bar{q} \rightarrow$

$g\gamma$ with longitudinally polarized colliding protons.

The squared modules of matrix element, averaged over the spin of the final particles, with longitudinally polarized colliding proton is:

$$|\bar{M}|^2 = \frac{8\alpha_e\alpha_s e_q^2}{9}\frac{(\hat{u}^2 + \hat{t}^2)}{\hat{t}\hat{u}}(1 - \lambda_1\lambda_2).$$

At the parton level, the DS of the subprocess is determined by the following expression:

$$\frac{d\hat{\sigma}_{LO\_POL.}(q\bar{q} \to g\gamma)}{d\hat{t}} = \frac{1}{16\pi\hat{s}^2}|\bar{M}|^2.$$

At the parton level, the expression for the double spin asymmetry of annihilation of quark-antiquark pair subprocess is:

$$\hat{A}_{LL} = -\lambda_1\lambda_2.$$

6. DS of subprocess of bremsstrahlung $qq \to qq\gamma$ with longitudinally polarized colliding protons.

The Feynman diagrams, matrix elements and Mandelstam invariants of the subprocess of bremsstrahlung $qq \to qq\gamma$ with longitudinally polarized colliding protons have the same form as for the case unpolarized.

To account for quark polarization, the expression (2) was used for the product of four-dimensional spinors.

Analysis of the total cross-section shows that the effect of polarization is consistent across all energy ranges. The dependence of the DS on the photon's transverse momentum (p_T) indicates that polarization has a significant impact at small p_T. As p_T increases, its influence decreases.

Summarizing the results, it can be noted that over 50% of the DS for prompt photon production comes from the quark-gluon Compton scattering subprocess ($qg \to q\gamma$), approximately 40% from quark-antiquark annihilation ($q\bar{q} \to g\gamma$), and less than 0.03% from bremsstrahlung ($qq \to qq\gamma$). At NICA energies the Compton scattering subprocess remains dominant.

The polarization of colliding particles enhances or weakens the DS depending on the sign of P_1P_2. For positive P_1P_2, the DCS of bremsstrahlung increases, while the cross-section for quark-antiquark annihilation decreases. For negative P_1P_2, the opposite occurs.

Polarization significantly affects small p_T values for Compton scattering ($qg \to q\gamma$) and quark-antiquark annihilation ($q\bar{q} \to g\gamma$). For bremsstrahlung ($qq \to qq\gamma$), its influence is more pronounced at large p_T.

Bremsstrahlung is an electromagnetic process where a photon interacts with a particle's electric field. Quark-antiquark annihilation is a strong interaction process linked to color charge. Polarization effects in bremsstrahlung arise from interference, while in annihilation, they result from angular momentum conservation.

Polarization has a stronger impact at high collision energies, as relativistic protons become more sensitive to photon and gluon fields. Its effect is maximal at small p_T and diminishes as p_T increases.

The third chapter is devoted to the study of one-loop contributions to Compton scattering of quark-gluon and annihilation of quark-antiquark pair subprocesses.

1. DS of Compton scattering of quark-gluon scattering $qg \to q\gamma$ subprocess with unpolarized colliding protons.

The DS of the subprocess $qg \to q\gamma$ at the parton level was defined as[13]:

$$|\bar{M}|^2 = \frac{0.0012\alpha_e \alpha_s^3 e_q^2 (\hat{s}^3 + \hat{s}^2\hat{u} + \hat{s}\hat{u}^2 + \hat{u}^3)}{\hat{u}^2(\hat{s} + \hat{u})}$$

and

$$\frac{d\hat{\sigma}_{NLO}(qg \to q\gamma)}{d\hat{t}} = \frac{1}{16\pi\hat{s}^2}|\bar{M}|^2.$$

Figure 8(a,b,c,d) shows the dependences of the ratio $R = d\sigma_{NLO}(qg \to q\gamma)/d\sigma_{LO}(qg \to q\gamma)$ on the sum of energy of colliding particles $\sqrt{s}$, transverse momentum p_T, prompt photons rapidity y and x_T at $\sqrt{s}$=10 GeV.

---

13 Alizade M.R., Akhmedov A.I. Arbuzov A.B. Differenchialnoye secheniye rojdeniya pryamikh fotonov v proton-proton stolknovenii s uchyotom odnopetlevogo vklada na samoenergiyu fotona v KXD // Proceedings of the 2nd International Science and Technology Conference, Baku Engineering University, – Baku: Azerbaijan, – 2021. November 26-27, – p.212-216, (in Russian).

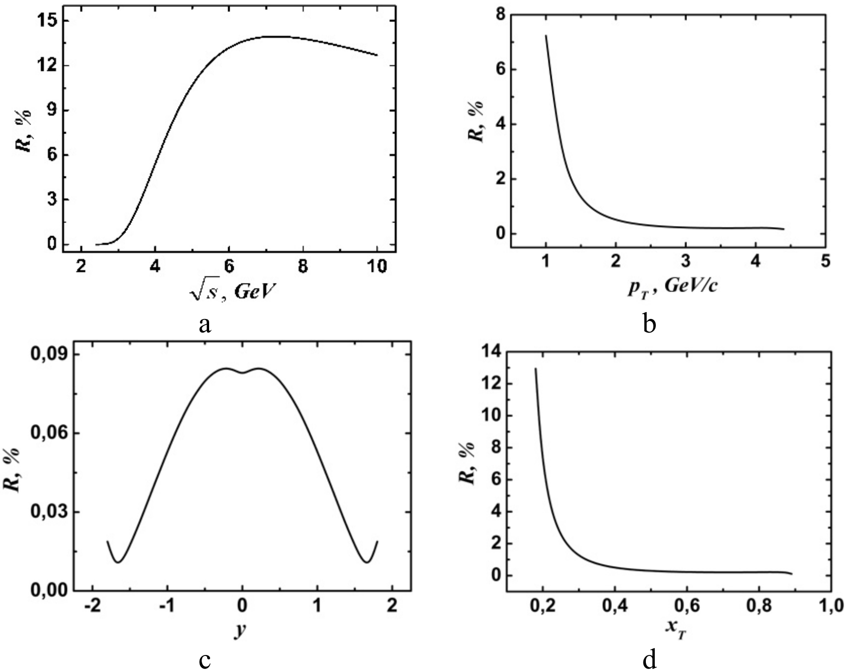

Figure 8 (a, b, c, d).

Figure 8(a,b,c,d) shows the dependence of the ratio of DS calculated at LO and NLO, $R = d\sigma_{NLO}/d\sigma_{LO}$, on the total energy of colliding particles ($\sqrt{s}$), photon transverse momentum (p_T), rapidity (y), and x_T parameter at $\sqrt{s} = 10$ GeV.

The dependence of R on kinematic parameters confirms that higher-order corrections play a key role in describing the process, especially at high parton energies, consistent with pQCD predictions.

2. DS of subprocess of annihilation of quark-antiquark pair $q\bar{q} \to g\gamma$ with unpolarized colliding protons.

The square of the modulus of the matrix element for one loop correction of this subprocess, calculated with used dimensional regularization and averaged over the spins of the initial particles.

Figure 9(a,b) shows the dependence of the ratio $R = d\sigma_{NLO}\,(q\bar{q} \to g\gamma)/d\sigma_{LO}(q\bar{q} \to g\gamma)$ at the hadronic level on the sum of energy of colliding protons and the transverse momentum of prompt photons p_T.

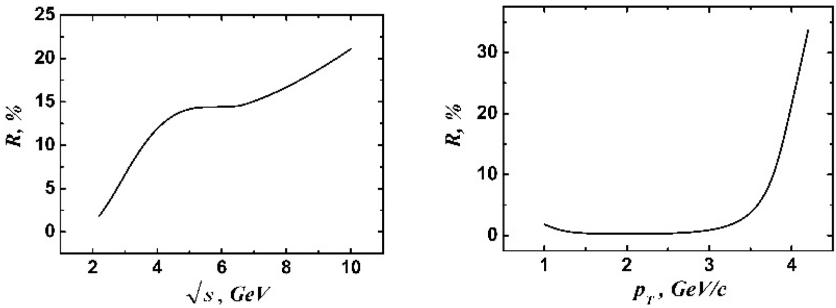

a b

Figure 9 (a, b).

Comparison of LO and NLO shows that the LO contribution is proportional to $\alpha_s\alpha$, while the NLO contribution is proportional to $\alpha_s^2\alpha$. NLO calculations include additional Feynman diagrams and higher-order corrections, improving the accuracy of process description. The interference term is proportional to $\alpha_s^2\alpha\log(s/M^2)$, where M is the renormalization scale. At small x, the cross-section increases, making NLO calculations more significant.

3. DS of the subprocess of Compton scattering of quark-gluon $qg \to q\gamma$ with longitudinally polarized colliding protons.

The matrix elements and Mandelstam invariants will be identical, with the case without polarization. Given the polarization of the initial particles as (2), for the square of the matrix element averaged over the spin of the initial particles for one loop correction of the subprocess $qg \to q\gamma$ with the applied dimensional regularization, we obtain:

$$|\bar{M}|^2 = -\frac{8\alpha_e\alpha_s e_q^2}{9}\left(\frac{\hat{s}}{\hat{u}}(1 - 2\lambda_1\lambda_2 + \lambda_2^2) + \frac{\hat{u}}{\hat{s}}(1 + 2\lambda_1\lambda_2 + \lambda_2^2)\right).$$

For the DS of the subprocess $qg \to q\gamma$ at the parton level following expression was obtained:

$$\frac{d\hat{\sigma}_{NLO}(qg \to q\gamma)}{d\hat{t}} = \frac{1}{16\pi\hat{s}^2}|\bar{M}|^2.$$

To calculate the DS at the hadronic level, it is necessary to take into account the polarized PDF for the NLO (2).

Figure 10(a,b) shows the dependence of the ratio $R =$

$d\sigma_{NLO\_POL}(qg \to q\gamma)/d\sigma_{NLO}(qg \to q\gamma)$ on the sum of the energy of colliding protons $\sqrt{s}$ and the transverse momentum p_T of prompt photons.

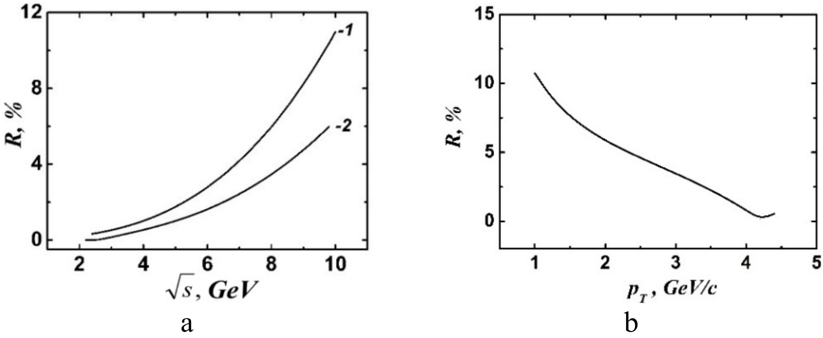

Figure 10 (a, b).

Figure 10(a) shows the dependence of the DS calculated by the NLO at $P_1 \cdot P_2 = -0.81$, as can be seen, the effect of polarization on the NLO calculations becomes significant at high energies of the colliding particles.

From Figure 10(a), it is evident that the effect of polarization on NLO becomes significant at high energies. Comparing LO and NLO, it is clear that polarization has a stronger impact on NLO than on LO (Figures 8 and 10). An explanation of this is given in section 3.2.

4. DS of the annihilation of quark-antiquark pair subprocess $q\bar{q} \to g\gamma$ with longitudinally polarized colliding particles.

The matrix elements and Mandelstam invariants remain similar to the unpolarized case. Taking into account the polarization of the initial particles, according to (2), for the square of the matrix element averaged over the spin of the initial particles in the case of a one loop correction of the subprocess $\bar{q} \to g\gamma$, applying dimensional regularization, we obtain:

$$|\bar{M}|^2 = -(\alpha_s e^2 e_q^2 (1 - \lambda_1\lambda_2)(\alpha_s^2(0.0004\hat{s}^2 + 0.0008\hat{s}\hat{t} +$$
$$+0.0008\hat{t}^2) + 0.001\alpha_s\hat{s}^2\hat{t}^2 + 0.0006\hat{s}^4\hat{t}^2)/(\hat{t}(\hat{s} + \hat{t})).$$

For the DS of the $q\bar{q} \to g\gamma$ subprocess at the parton level, taking into account the proton polarization was obtained:

$$\frac{d\hat{\sigma}_{NLO}(q\bar{q} \to g\gamma)}{d\hat{t}} = \frac{1}{16\pi\hat{s}^2}|\bar{M}|^2.$$

Figure 11(a,b) shows the dependences of the ratio $R = d\sigma_{NLO}(q\bar{q} \to g\gamma)/d\sigma_{LO}\,(q\bar{q} \to g\gamma)$ on the energy of colliding protons and the transverse momentum of prompt photons p_T at $\sqrt{s}$ =10 GeV.

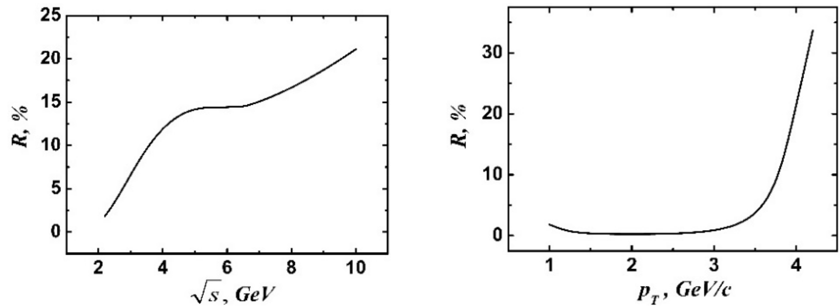

a b

Figure 11 (a, b).

From Figure 11(a), it is evident that R increases with $\sqrt{s}$, confirming the importance of NLO at high energies.

Figure 11(b) shows that the NLO contribution reaches up to 30% at large p_T.

Explanations of these are given in section 3.2.

The fourth chapter is devoted to the study of the contributions of radiation corrections 1. $qg \to qg\gamma$, 2. $qg \to q\gamma\gamma$, 3. $q\gamma \to qg\gamma$, 4. $g\gamma \to q\bar{q}\gamma$ and 5. $q\gamma \to q\gamma$ to the DS of the subprocess of Compton scattering of quark-gluon and the contributions of radiative corrections: 1. $q\bar{q} \to g\gamma\gamma$, 2. $q\bar{q} \to gg\gamma$ and 3. $q\bar{q} \to q\bar{q}\gamma$ to the DS of subprocess of annihilation of quark-antiquark pair of prompt photon production[14].

[14] Alizada M.R., Ahmadov A.I. Radiation correction to Compton scattering of quark-gluon and annihilation of quark-antiquark pair processes of prompt photon production in proton-proton collisions at high energies // Transactions of Azerbaijan National Academy of Sciences, Physics and astronomy, – Baku: – 2023, N 2, – c.3-10.

1. Radiation corrections to Compton scattering of quark-gluon $qg \to g\gamma$ subprocess with unpolarized colliding particles.

The square of the modulus of the matrix elements of subprocesses: $qg \to qg\gamma$, $qg \to q\gamma$, $q\gamma \to qg\gamma$, $g\gamma \to q\bar{q}\gamma$ and $q\gamma \to q\gamma$ was determined [15],[16]. In the parton level, the DS will determine as shown in below:

$$\frac{d\hat{\sigma}}{d\hat{t}} = \frac{\hat{s}_1}{16\pi^2\hat{s}^4}|\bar{M}|^2. \tag{6}$$

Futhere expressions (1) and (2) are used for the transition to the hadronic level.

2. Radiation corrections to annihilation of quark-antiquark pair subprocess $q\bar{q} \to g\gamma$ with unpolarized colliding protons.

The square of the modulus of the matrix element of the subprocess $q\bar{q} \to g\gamma\gamma$, $q\bar{q} \to gg\gamma$ and $q\bar{q} \to q\bar{q}\gamma$ was determined.

The DS of the subprocess will be determined by formula (6) for the parton level, and expressions (1) and (2) are used for the transition hadronic level.

Figure 12(a,b) shows the dependences of the DS of the radiative corrections to Compton scattering of quark-gluon and to annihilation of quark-antiquark pair on the transverse momentum p_T.

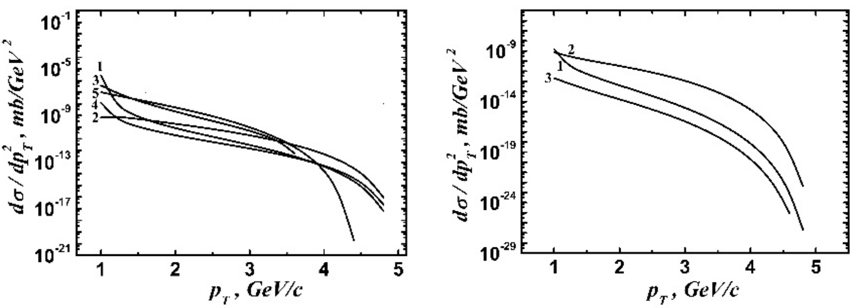

a b

Figure 12 (a, b).

[15] Alizada M.R. Ahmadov A.I., Arbuzov A.B. Prompt photon production in subprocesses $qg \to q\gamma$ and $q\gamma \to q\gamma$ of compton scattering in proton–proton collision at NICA energies // Physics of Particles and Nuclei Letters, – Moscow: Dubna: – 2024, Vol. 21, No. 2, pp. 85–89.

The following relation is true for the contributions of radiative corrections to Compton quark-gluon scattering:

$$\frac{d\sigma(qg \to qg\gamma)}{dp_T^2} > \frac{d\sigma(q\gamma \to q\gamma)}{dp_T^2} > \frac{d\sigma(qg \to g\gamma\gamma)}{dp_T^2}$$
$$> \frac{d\sigma(g\gamma \to q\bar{q}\gamma)}{dp_T^2} > \frac{d\sigma(q\gamma \to qg\gamma)}{dp_T^2}.$$

The following relation is true for the contributions of radiative corrections to annihilation of quark-antiquark pair:

$$\frac{d\sigma(q\bar{q} \to gg\gamma)}{dp_T^2} > \frac{d\sigma(q\bar{q} \to g\gamma\gamma)}{dp_T^2} > \frac{d\sigma(q\bar{q} \to q\bar{q}\gamma)}{dp_T^2}.$$

3. Radiation corrections to Compton scattering of quark-gluon $qg \to q\gamma$ subprocess with longitudinally polarized colliding protons.

The squared matrix element for the subprocess $q\gamma \to q\gamma$, averaged over the spins of initial particles, is given by:

$$|\bar{M}|^2 = -\frac{8e^2e_q^2}{27}\left(\frac{\hat{s}}{\hat{u}}(1 - 2\lambda_1\lambda_2 + \lambda_2^2) + \frac{\hat{u}}{\hat{s}}(1 + 2\lambda_1\lambda_2 + \lambda_2^2)\right).$$

The DS for the subprocess $q\gamma \to q\gamma$ with polarization is:

$$\frac{d\hat{\sigma}_{POL.}(q\gamma \to q\gamma)}{d\hat{t}} = -\frac{\pi\alpha_e^2 e_q^2}{4\hat{s}^2 e^2}|\bar{M}|^2.$$

The relationship between DS with and without polarization is:

$$\frac{d\hat{\sigma}_{POL.}}{d\hat{t}} = \frac{\left(\hat{s}^2(1 - 2\lambda_1\lambda_2 + \lambda_2^2) + \hat{u}^2(1 + 2\lambda_1\lambda_2 + \lambda_2^2)\right)}{(\hat{s}^2 + \hat{u}^2)}\frac{d\hat{\sigma}}{d\hat{t}}.$$

The double spin asymmetry calculated at the parton level for the subprocess $q\gamma \to q\gamma$ is as (5).

At the hadron level, the double-spin asymmetry is expressed as:

$$A_{LL} = P_1P_2\frac{\int \Delta G_{r_1/h_1}(x_1)\Delta G_{r_2/h_2}(x_2)\hat{A}_{LL}d\hat{\sigma}_{\text{unpol.}}\,dx_1\,dx_2}{\int G_{r_1/h_1}(x_1)G_{r_2/h_2}(x_2)d\hat{\sigma}_{\text{unpol.}}\,dx_1\,dx_2},$$

where P_1 and P_2 are the polarization orders of the colliding protons,

$\Delta G_{r_i/h_i}(x) = G^{\uparrow}_{r_i/h_i}(x) - G^{\downarrow}_{r_i/h_i}(x)$ is the difference of PDF for different polarization directions, $G_{r/h}(x) = G^{\uparrow}_{r/h}(x) + G^{\downarrow}_{r/h}(x)$ is the total parton distribution.

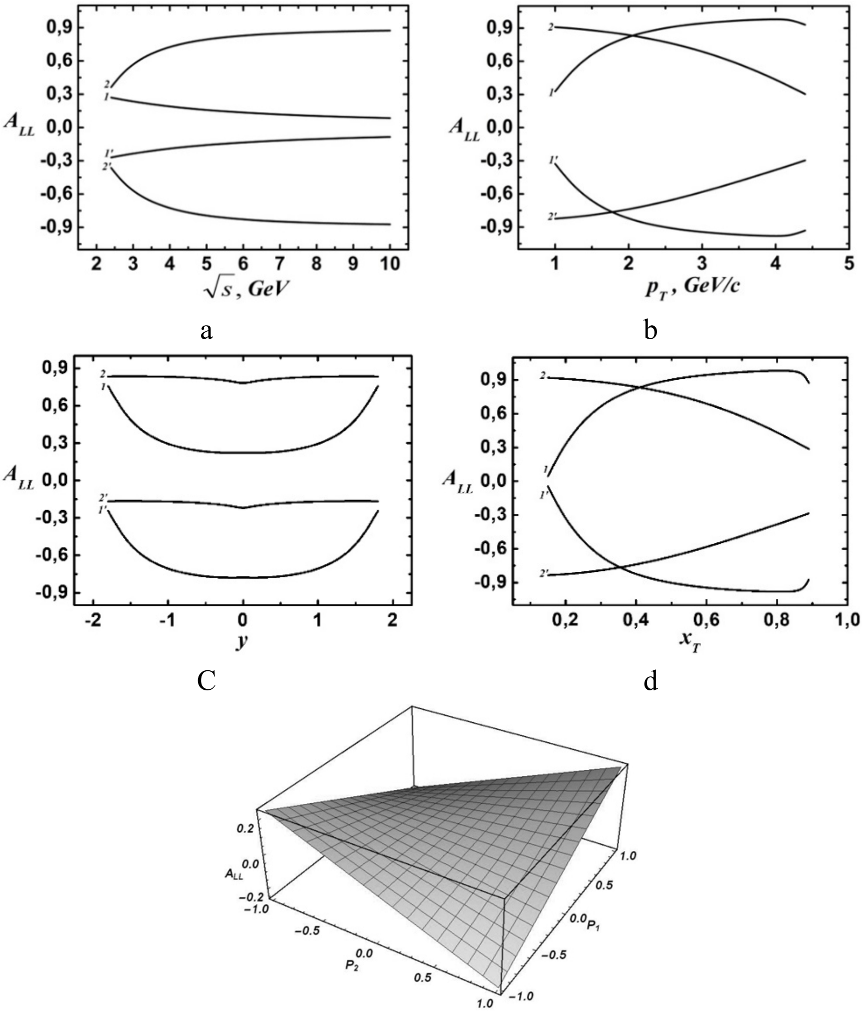

Figure 13 (a, b, c, d, e).

Figure 13(a,b,c,d,e) shows the dependence of the double spin asymmetry for the subprocesses $qg \to q\gamma$ and $q\gamma \to q\gamma$ on the energy of colliding particles ($\sqrt{s}$), the transverse momentum of photons (p_T), rapidity (y), and the parameter x_T for various polarization orders P_1, P_2[13].

From Figure 13(a), it is evident that the asymmetry increases with $\sqrt{s}$ when $P_1, P_2 = 0.9, -0.9$ (curve 1) and decreases when $P_1 = P_2 = \pm 0.9$ (curve 2).

The dependence of asymmetry on p_T and x_T shows that it decreases with increasing parameters when $P_1, P_2 = 0.9, -0.9$, but increases when $P_1 = P_2 = \pm 0.9$.

The 3D plot (Figure 13(e)) shows that the maximum asymmetry occurs when P_1 and P_2 have opposite signs. This aligns with theoretical predictions, as opposite polarization directions enhance spin effects.

4. Radiation corrections to annihilation of quark-antiquark pair $qg \to g\gamma$ subprocess with longitudinally polarized colliding protons.

Figure 14 shows the dependence of the double spin asymmetry (A_{LL}) for the subprocesses $q\bar{q} \to gg\gamma$, $q\bar{q} \to g\gamma\gamma$, and $q\bar{q} \to \gamma\gamma$ on the product of the polarization orders of colliding protons.

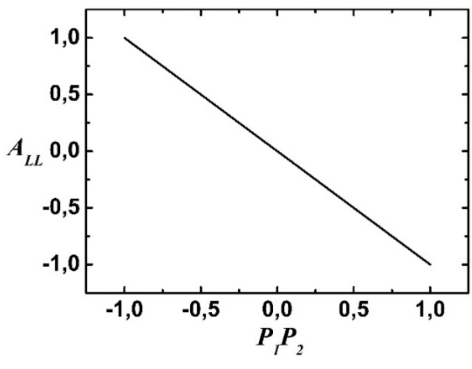

Figure 14.

As seen, A_{LL} decreases with increasing P_1P_2.

Figure 15(a,b,c,d) presents the dependence of A_{LL} for the subprocess $q\bar{q} \to q\bar{q}\gamma$ on the energy of colliding protons ($\sqrt{s}$), the transverse momentum of photons (p_T), rapidity (y), and the parameter x_T

for various values of P_1P_2.

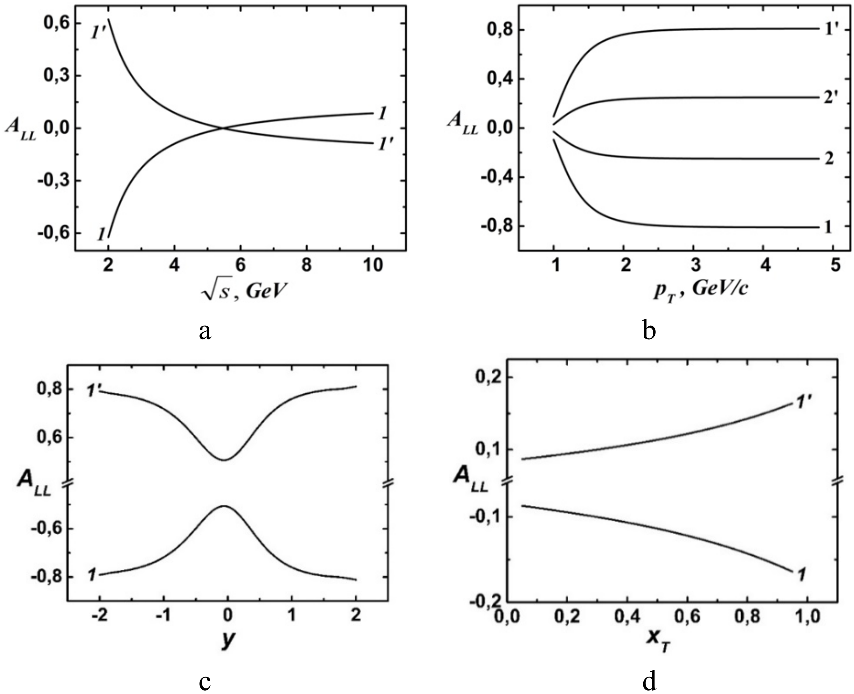

Figure 15 (a, b, c, d).

From Figure 15(a), it is evident that polarization has a significant effect at low energies. At $\sqrt{s} = 5.5$ GeV, the DS calculated with and without polarization coincide, but with increasing p_T, the cross-section becomes smaller for $P_1P_2 < 0$ and larger for $P_1P_2 > 0$ compared to the unpolarized case.

The double spin asymmetry increases (for $P_1P_2 < 0$) or decreases (for $P_1P_2 > 0$) with increasing p_T and reaches saturation at a certain p_T (Figure 15(b)). The saturation value and p_T increase with growing $|P_1P_2|$.

Figure 15(c) shows that A_{LL} in the interval $y \in [-2,0]$ increases for $P_1P_2 < 0$ (curve 1) and decreases for $P_1P_2 > 0$ (curve 1'). At $y = 0$, A_{LL} reaches its maximum for $P_1P_2 < 0$ and minimum for $P_1P_2 > 0$.

Figure 15(d) shows that A_{LL} decreases (curve 1) or increases (curve 1') with increasing x_T. For the subprocess $qg \to q\gamma$, A_{LL} weakly depends on the polarization of initial particles. The maximum A_{LL} is achieved when P_1 and P_2 have opposite signs.

The contribution of radiative corrections to Compton scattering $qg \to q\gamma$ is more significant than that for quark-antiquark annihilation $q\bar{q} \to g\gamma$.

The fifth chapter is devoted to the study of the production of prompt photons in the proton-antiproton collision.

In proton-proton collisions, the following subprocesses take place for the subprocess of Compton scattering of quark-gluon: 1. $u_v g \to u_v\gamma$, 2. $u_s g \to u_s\gamma$, 3. $\bar{u}_s g \to \bar{u}_s\gamma$, 4. $d_v g \to d_v\gamma$, 5.$d_s g \to d_s\gamma$ and 6. $\bar{d}_s g \to \bar{d}_s\gamma$. For annihilation of quark-antiquark pair subprocess, the following subprocesses will be possible: 1. $u_v\bar{u}_s \to g\gamma$, 2. $d_v\bar{d}_s \to g\gamma$, 3. $u_s\bar{u}_s \to g\gamma$ and 4. $d_s\bar{d}_s \to g\gamma$ where u_v, d_v are valence, u_s, d_s are sea quarks, correspondingly.

In the proton-antiproton collision, the subprocesses, as in the proton-proton collision, are Compton scattering of quark-gluon $qg \to q\gamma$ and annihilation of quark-antiquark pair $q\bar{q} \to g\gamma$. In the proton-antiproton collision, the following subprocesses occur in the subprocess of Compton scattering of quark-gluon: 1. $u_v g \to u_v\gamma$, 2. $\bar{u}_v g \to \bar{u}_v\gamma$, 3. $u_s g \to u_s\gamma$, 4. $\bar{u}_s g \to \bar{u}_s\gamma$, 5. $d_v g \to d_v\gamma$, 6. $\bar{d}_v g \to \bar{d}_v\gamma$, 7.$d_s g \to d_s\gamma$ and 8. $\bar{d}_s g \to \bar{d}_s\gamma$, and in annihilation of quark-antiquark pair subprocess the following subprocesses occur: 1. $u_v\bar{u}_v \to g\gamma$, 2. $u_s\bar{u}_s \to g\gamma$, 3. $u_v\bar{u}_s \to g\gamma$, 4. $u_s\bar{u}_v \to g\gamma$, 5. $d_v\bar{d}_v \to g\gamma$, 6. $d_s\bar{d}_s \to g\gamma$, 7.$d_v\bar{d}_s \to g\gamma$ and 8. $d_s\bar{d}_v \to g\gamma$.

1. DS of proton-antiproton collision with unpolarized colliding protons and antiprotons.

Figure 16(a,b,c,d,e) shows the dependence of the DS of prompt photons production in proton-antiproton collisions $p\bar{p} \to \gamma X$ on the sum of the energies of the colliding particles $\sqrt{s}$, the transverse momentum of the prompt photonsp_T, the cosine of scattering angle, the rapidity y and x_T prompt photon at $\sqrt{s}$ =10 GeV[16].

[16] Alizada M.R. Prompt photon production in proton-proton and proton-antiproton collisions // Abstract book of XXV National Scientific conference (NASCO) of PhD students and young researchers, Baku: – 2022, 23-24 November, – s.67-71.

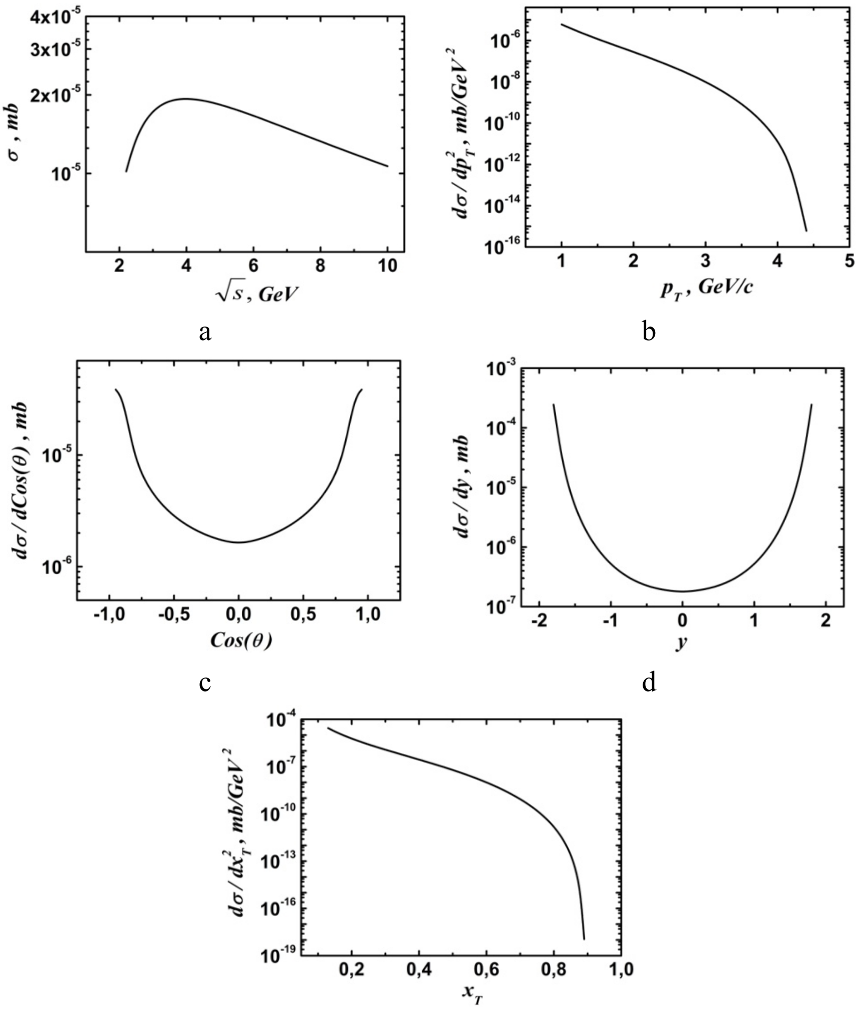

e

Figure 16 (a, b, c, d, e).

The dependence of the DS of the process $p\bar{p} \to \gamma X$ on $\sqrt{s}$ is higher than that for $pp \to \gamma X$ (Figure 2(a), Figure 4(a), Figure 6(a)). This is explained by differences in the quark composition of protons and antiprotons.

From Figure 16(b), it is evident that the DS decreases with increasing p_T. Photons with small p_T have a higher probability of being detected than those with large p_T.

The dependencies of the DS on the cosine of the scattering angle ($\cos\theta$) and rapidity (y) are symmetric about the point $\cos\theta = y = 0$. The maximum value is achieved near the boundaries of the intervals of $\cos\theta$ and y (Figure 16(c,d)).

The dependence of the DS on x_T is similar to its dependence on p_T (Figure 16(e)).

Figure 17(a,b) shows the dependence of the ratio $R = d\sigma(p\bar{p} \to \gamma X)/d\sigma(pp \to \gamma X)$ of DS with unpolarized colliding particles on the sum of the energy of colliding particles $\sqrt{s}$ (a) and on the transverse momentum of the production of prompt photon p_T (b) at $\sqrt{s}$ =10 GeV.

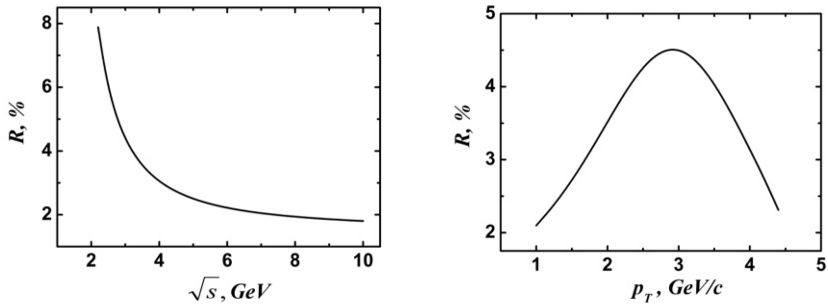

a b

Figure 17 (a, b).

As can be seen from Figure 17(a), the dependence of R on the sum of energy of colliding proton $\sqrt{s}$ decreases with increasing sum of energy od colliding proton and asymptotically approaches 1.66. It is known that the value of the ratio R of the dependence of the DS of proton-proton $pp \to \gamma X$ and proton-antiproton $p\bar{p} \to \gamma X$ collisions on the sum of energies of colliding protons $\sqrt{s}$ at LHC and Tevatron energies is equal to 1. At high energies it makes no difference whether the collision is proton-proton or proton-antiproton. At NICA energies the processes $pp \to \gamma X$ and proton-antiproton $p\bar{p} \to \gamma X$ can also be considered the same.

2. DS of the proton-antiproton collision with longitudinally polarized colliding protons and antiprotons.

The Feynman diagrams, the Mandelstam invariants and matrix elements remain unchanged for the process of formation of a prompt photon in the proton-antiproton collision taking into account polarization of proton and antiproton. Polarizations of colliding protons and antiprotons are taken into account as in (2) and (3).

Longitudinal polarization of antiprotons is accounted for as

$$\upsilon(p_2)\bar{\upsilon}(p_2) = \frac{1}{2}\hat{p}_2(1 + \gamma_5\lambda_2),$$

where $\lambda_{(2)}$ *is* the helicity of the initial antiquark.

Figure 18(a,b,c,d,e) shows the dependence of the DS of the process $p\bar{p} \to \gamma X$ taking into account the polarization of colliding protons and antiprotons at P_1, P_2=0.9, -0.9 (curve 1) and at P_1=P_2=±0.9 (curve 2) from the sum of energy of colliding particle $\sqrt{s}$ (a), transverse momentum of prompt photonsp_T (b), cosine of the scattering angle (c), rapidity at prompt photons (d), and x_T (e) at $\sqrt{s}$ =10 GeV.

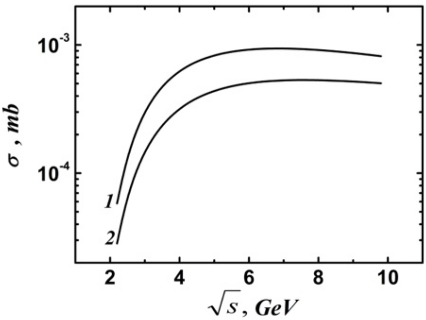

a

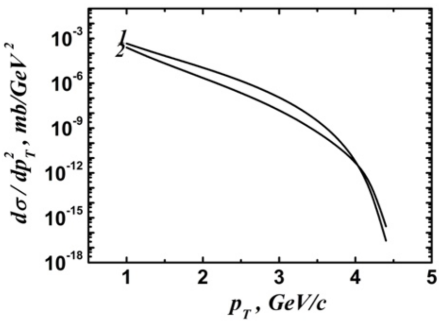

b

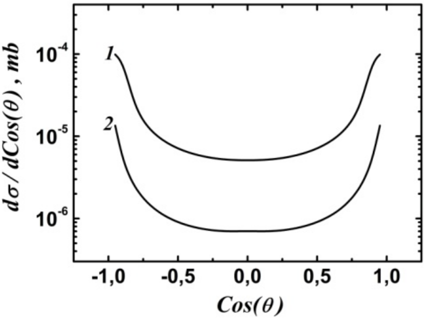

c

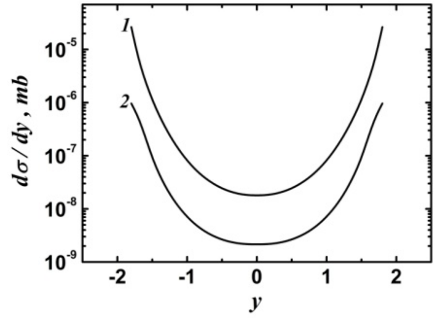

d

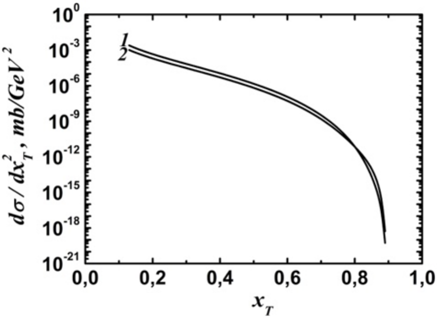

e

Figure 18 (a, b, c, d, e).

The DS of the quark-antiquark annihilation subprocess depends on the sign of P_1P_2: it can increase or decrease. The double spin asymmetry A_{LL} linearly depends on P_1P_2 and is symmetric with respect to changes in the signs of P_1 and P_2, i.e., $A_{LL}(-P_1, P_2) = A_{LL}(P_1, -P_2)$. This applies to both proton-proton and proton-antiproton collisions.

CONCLUSIONS

1. The production of prompt photons in the proton-proton collision mainly occurs in Compton scattering of quark-gluon $qg \to q\gamma$, annihilation of quark-antiquark pair $q\bar{q} \to g\gamma$ and bremsstrahlung $qq \to qq\gamma$ subprocesses. The DS of the prompt photon production process consists of more than 50% of the DS of Compton scattering of quark-gluon and about 43% of the DS of annihilation of quark-antiquark pair and less than 0.03% of the DS of bremsstrahlung. Compton scattering of quark-gluon $qg \to q\gamma$ subprocess is the dominant subprocess. In the NICA energies, gluons in the proton are as large a majority as in the LHC and Tevatron energies.
2. In proton-proton collisions the dependence of the cross-section for prompt photon production in subprocesses of Compton scattering of quark-gluon, annihilation of quark-antiquark pair, and bremsstrahlung on kinematic parameters is as follows: the total

cross-section for prompt photon production increases with the rise in the sum of energy of colliding particles, the DS decreases with the increase in the transverse momentum of photons, and photons are scattered at angles close to the particle collision axis (16 and 164 degrees).

3. Longitudinal polarization of colliding protons does not change the character of the dependence of the DS of the subprocesses of Compton scattering of quark-gluon, annihilation of quark-antiquark pair and bremsstrahlung. The longitudinal polarization of colliding particles differently affects the values of the DS of Compton scattering of quark-gluon, annihilation of quark-antiquark pair, and bremsstrahlung. At the same directionality of polarization of colliding particles the DS of the subprocesses of Compton scattering of quark-gluon and annihilation of quark-antiquark pair decreases, and the DS of bremsstrahlung increases. The polarization of colliding particles strongly affects annihilation of quark-antiquark pair subprocess. The effect of proton polarization on the DS is indicated by the interaction of parton spins.

4. The DS of Compton scattering of quark-gluon and annihilation of quark-antiquark pair calculated at the next-to-leading order are about 15% and 30%, correspondingly, of those calculated at the leading order. The longitudinal polarization of colliding protons strongly affects the DS calculated next-to-leading order than the leading order. The contribution of the Next-to-leading calculation to the DS is significant at high energies of colliding particles.

5. The contributions of radiative corrections to Compton scattering of quark-gluon subprocess sum up to about 30% of the main process, and the contributions of radiative corrections to annihilation of quark-antiquark pair sum up to about 5%. The contributions of radiative corrections to the DS of Compton scattering of quark-gluon $qg \to q\gamma$ subprocess are more significant than the contributions of corrections to the DS of annihilation of quark-antiquark pair $q\bar{q} \to g\gamma$ subprocess, which indicates a stronger interaction of the quark with the strong field quantum gluon than with the electric field quantum photon.

6. The DS of prompt photon production in the proton-antiproton collision process is larger than in the proton-proton collision process. At NICA energies, the ratio of the DS of proton-antiproton and proton-proton collisions is 1.66, which allows to consider the proton-proton and proton-antiproton collisions identical. The effect of sea quarks on the proton-antiproton DS decreases at high energies. The influence of polarization on the DS of colliding particles in the proton-antiproton collision is significant.

7. By nature, the calculated dependences of the DS of the subprocesses on the kinematic parameters agree with the experimental results of the LHC, Tevatron. The use of the parton distribution function CT14QED in the calculations of the DS in NICA energies gives acceptable results. However, a comparison of the theoretical calculations with the experimental results of NICA is required to fully validate the choice.

Scientific works published on the subject of the dissertation work:

1. Alizade, M.R., Akhmedov, A.I., Arbuzov, A.B. Issledovaniye pod prochessov $qg \rightarrow q\gamma$ i $q\bar{q} \rightarrow g\gamma$ rojdeniya pryamikh fotonov pri proton-protonnom stolknovenii // – Baku: Transactions of Azerbaijan National Academy of Sciences, Physics and astronomy, – 2021, 5, – p.11-19, (in Russian).

2. Alizade, M.R., Akhmedov, A.I., Arbuzov, A.B. Differenchialnoye secheniye rojdeniya pryamikh fotonov v proton-proton stolknovenii s uchyotom odno-petlevogo vklada na samoenergiyu fotona v KXD // Proceedings of the 2nd International Science and Technology Conference, Baku Engineering University, – Azerbaijan: Baku: – November 26-27, – 2021, – p.212-216 (in Russian).

3. Alizada, M.R., Ahmadov, A.I., Arbuzov, A.B. Prompt photons production in proton-proton collision at high energies // Abstract book of the 7th International conference MTP-2021, Modern Trends in Physics, Baku State University, – Azerbaija: Baku: –

2021. December 15-17, – p. 22-23.

4. Alizada, M.R., Ahmadov, A.I., Arbuzov, A.B. Prompt photons production in proton-proton collision at high energies // Proceedings of the 7th International conference MTP-2021, Modern Trends in Physics, Baku State University, – Azerbaijan: Baku: 1, December 15-17, – 2021, – p.142-145.

5. Alizada, M.R., Ahmadov, A.I., Arbuzov, A.B. Study of polarization effects in prompt photon production // – Baku: Transactions of Azerbaijan National Academy of Sciences, Physics and astronomy, – 2022, 2, – p.9-16 (in Russian).

6. Alizade, M.R. Rojdeniya pryamikh fotonov pri proton-proton stolknovenii v energiyakh NICA $\sqrt{s}$=10 GeV // Azerbaycan Respublikasi Tehsil Nazirliyi, Baki Dovlet Universiteti Magistrantlarin ve genc tedgigatchilarin "SHUSHA ILI"-ne hesr olunmush "Fizika ve Astronomiya Problemleri" adlı XXII Umumrespublika elmi konferansi, – Baku: – May 20, – 2022, – p. 13-14 (in Russian).

7. Alizade, M.R., Akhmedov A.I. Rozdenie fotonov v prochessakh $\pi^+\pi^- \to \gamma\rho^0$, $\rho^0 \to \pi^+\pi^-\gamma$ // Umummilli Lider Heyder Eliyevin anadan olmasinin 99-cu il donumune hesr olunmush Genc Tedgigatchilarin VI Beynelxalq Elmi Konfransi 29-30 Aprel 2022 Baki Muhendislik Universiteti, Khirdalan/Azerbaycan Dovlet Gomruk Komitesinin Akademiyasi, Sabunchu / Azerbaycan, Baki: – Aprel, – 2022. – s.41-45 (in Russian).

8. Alizada, M.R. Thermal photons production in proton-proton collision at high energies // LXXII International Conference "Nucleus-2022: Fundamental problems and applications", – Moscow: – 2022. July 11-16, – p.225.

9. Alizada, M.R. Prompt photon production in proton-proton and proton-antiproton collisions // Abstract book of XXV National Scientific conference (NASCO) of PhD students and young researchers, Baku: – November 23-24, – 2022, – s .67-71.

10. Alizada, M.R., Ahmadov, A.I. Thermal photons production in proton-proton collisions at high energies. Part I. Differential cross-sections of processes, calculated without and taking into account formfactor of mesons // – Baku: Azerbaijan Journal of

Physics “Fizika”, – 2023, XIX(1), Section En, – p.3-12.

11. Alizada, M.R., Thermal photons production in proton-proton collisions at high energies. Part II. Determination of dominant process of production of thermal photons // – Baku: Azerbaijan Journal of Physics “Fizika”, – 2023, XIX(1), Section En,, – p. 29-37.

12. Alizada, M.R., Ahmadov, A.I. Radiation correction to Compton scattering of quark-gluon and annihilation of quark-antiquark pair processes of prompt photon production in proton-proton collisions at high energies // – Baku: Transactions of Azerbaijan National Academy of Sciences, Physics and astronomy, – 2023, N 2, – с. 3-10.

13. Alizada, M.R. Thermal photons production in $\pi^+\pi^- \to \gamma\rho^0$, $\pi^\pm\rho^0 \to \gamma\pi^\pm$ and $\pi^+\pi^- \to \gamma\gamma$ processes // – Москва: News of the Russian Academy of Sciences, Physical Series, – 2023. 87(9), – p. 1226-1231

14. Ализаде, M.Р. Rojdeniye pryamikh fotonov v kvant khromodinamicheskom i elektrodinamicheskom komptonovskikh rasseyaniyakh // Magistrantlarin ve genc tedgigatchilarin “HEYDER ELIYEV ILI”–ne hesr olunmush Fizika ve astronomiya problemleri adlı XXIII Umumrespublika Elmi Konfransı BDU, – Bakı: – May 25 , – 2023, – s. 5-6. (in Russian).

15. Alizada, M. Effect of polarization of colliding protons on the differential cross-section of the sub-process of production of prompt photon in Compton scattering of quark-gluon, annihilation of quark-antiquark pair. // VII International scientific conference of young researcher, – Baku: 27-28 April, – 2023, – p. 84-86.

16. Alizada, M.R. Prompt photon production in bremsstrahlung from quark gluon plasma at $\sqrt{s}$=10 GeV energies // 21st Lomonosov Conference on Elementary Particle Physics, Moscow: Moscow State University, – Moscow: – August 24-30, – 2023, [Electronic resource] / URL:https://lomcon.ru/?page_id=1156, https://lomcon.ru/files/21LomCon/%d0%9f%d1%80%d0%b5%d0%b7%d0%b5%d0%bd%d1%82%d0%b0%d1%86%d0%b8%d0%b8/25.08_B/(8)ALIZADA__MR___PRSNTN.pdf.

17. Alizada, M.R., Ahmadov, A.I., Arbuzov, A.B. Prompt photon production in bremsstrahlung at NICA energies // 8th International conference MTP 2023, Modern Trends in Physics, – Azerbaijan: Baku: – November 30 – December 1, – 2023, – p. 65-66.
18. Alizada, M.R., Ahmadov, A.I., Arbuzov, A.B. Prompt photon production in the bremsstrahlung at NICA energies // – Baku: Journal of Physics & Space Sciences, Baku State University: – 2024, 1(2), – p. 43-49.
19. Alizada, M.R. Ahmadov, A.I., Arbuzov, A.B. Prompt photon production in sub-processes $qg \rightarrow q\gamma$ and $q\gamma \rightarrow q\gamma$ of compton scattering in proton–proton collision at NICA energies // – Moscow: Dubna: Physics of Particles and Nuclei Letters, – 2024, 21(2), – p. 85–89.
20. Alizada, M.R. Prompt photon production in bremsstrahlung from quark gluon plasma at $\sqrt{s}$=10 GeV energies // – Moscow: Bulletin of Moscow State University, Moscow: – 2024, 79(Suppl.1), – S39-S41.
21. Alizada, M.R. Ahmadov, A.I., Arbuzov, A.B. Contribution of the QED compton scattering subprocess to prompt photon production in collisions of longitudinally polarized protons at NICA energies // Physics of Particles and Nuclei Letters, – Moscow: – Dubna: – 2025, 22(2), – p. 6-17.

The defense will be held on 29 April 2025 at 15^{30} the meeting of the Dissertation council ED 2.19 of Supreme Attestation Commission under the President of the Republic of Azerbaijan operating at the Baku State University.

Address: Baku, Az 1148, Z. Khalilov str. 33, Baku State University.

Dissertation is accessible at the Library of Baku State University.

Electronic version of the abstract is available on the official website of the Baku State University.

Abstract was sent to the required addresses on 18 March **2025.**

Signed for print:	**27.02.2025**
Paper format:	**A5 (60×90 1/16)**
Volume:	**39810 char.**
Number of hard copies:	**20 units.**